



Influence of atmospheric forces on sea-surface fluctuations in Iraq marine water, northwest of Arabian Gulf

Ali Abdulridha Lafta¹

Received: 28 October 2020 / Accepted: 7 July 2021 / Published online: 3 August 2021
© Saudi Society for Geosciences 2021

Abstract

This study examines the response of a sea-surface at the Iraq marine water to changes in local meteorological elements [atmospheric pressure (AP), air temperature (AT), and wind field]. Harmonic analysis was conducted to extract the tidal part and nontidal part [meteorological tide or residual water level (RWL)] from the original water level data. The results showed relative changes in the meteorological tide between the seasons. The changes in the meteorological tide throughout the year correlated well with the changes in local meteorological forces. The statistical analysis results for RWL daily averages revealed that the annual range reaches 1.08 m with the maximum and minimum limits in summer and winter, respectively. The spectral analysis results indicated that the annual cycle of RWL accounts for only 21% of the total variance. Moreover, the variations in AP and AT strongly corresponded with their annual cycles. For wind stress components, the annual cycle in their spectrum was insignificant since the highest variance percentage coincided with other cycles, particularly with their high-band frequencies range. The regression analysis showed that during winter, the variations in RWL are mainly attributed to changes in AP, cross-shore wind stress (CSWS), and along-shore wind stress (ASWS), whereas during spring, the RWL variations are due to changes in CSWS, ASWS, and AP. Furthermore, in summer, the RWL variations are attributed to changes in AP, AT, and ASWS, whereas in autumn, the variations in the RWL are because of changes in AP, ASWS, and CSWS. Therefore, the results obtained could be beneficial for various activities in this important region of the Arabian Gulf.

Keywords Sea-surface · Meteorological tide · Harmonic analysis · Spectral analysis · Wind stress · Arabian Gulf

Introduction

Understanding the variations in sea level is crucial for several coastal activities, such as navigation safety, coastal infrastructures, and shoreline defense techniques. Identification of the sea level changes requires determining important forces that cause these variabilities. Sea level changes are mainly attributed to two principal forces, tidal (astronomical) and nontidal (Boon 2013; Zubier 2010; Zubier and Eyouni 2020). The contribution of these two forces in sea level variation is not constant and varies continuously. The time scale of the sea level variations in the coastal regions ranges from a few

minutes to several decades (Li and Han 2015; Pugh and Woodworth 2014; Willis et al. 2008).

Tide, caused by the mutual attraction and centrifugal forces of the sun, Earth, and moon system, is the most significant contributor to the sea level variations around the world. The main remarkable feature of a tide is its periodicity, which is a predictable parameter if appropriate techniques are applied (Boon 2013). In addition to the tidal force, oceanographic factors can contribute to sea level variations, which contain the effect of several forces such as seawater expansion/contraction, evaporation, and the density gradient due to the exchange between different water masses (Stewart 2009). Furthermore, sea level varies due to the fluctuation in the local atmospheric forces, such as atmospheric pressure (AP) and wind stress. Typically, sea level has an inverse relationship to AP (Saad et al. 2011); that is, sea level rises when AP drops and vice versa, known as an inverse barometer.

Moreover, the atmosphere drives the ocean by transferring momentum through wind stress. Wind stress represents the force exerted by the wind on the sea-surface, which acts by

Responsible Editor: Zhihua Zhang

✉ Ali Abdulridha Lafta
ali.lafta@uobasrah.edu.iq

¹ Department of Marine Physics, Marine Science Center, University of Basrah, Basrah, Iraq

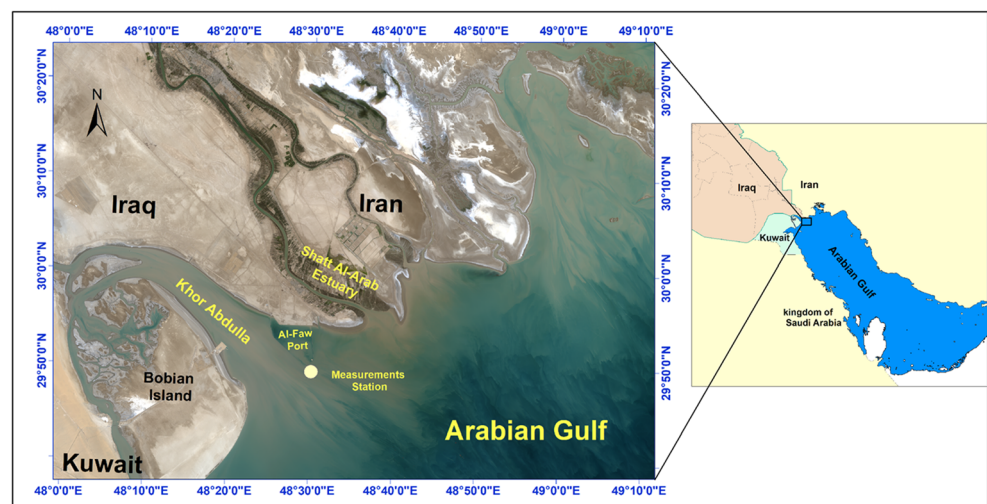
driving the water in the same direction as the wind. Hence, the sea-surface will rise or fall due to this interaction (Pugh and Woodworth 2014). Therefore, sea level responses to wind stress depend on the magnitude and directions of the wind. The main factors controlling the response of sea level to the wind stress are seawater flow direction, the period of wind blowing, and the dimensions of the water basin (Stewart 2009).

Iraq marine water is situated at the northwest tip of the Arabian Gulf (Fig. 1). The Arabian Gulf is a semi-enclosed water body with a length, maximum width, and mean depth reaching 990 km, 370 km, and 36 m, respectively (Reynolds 1993).

The Arabian Gulf is one of the main waterways of oil transport and oil industries in the world. Therefore, it receives very high attention from researchers in various scientific fields, in particular, oceanographic studies (Sadrinasab and Kämpf 2004; Kämpf and Sadrinasab 2006; Allothman and Ayhan 2010; AlOsairi et al. 2011; Siddig et al. 2019; Ranjbar et al. 2020). Meanwhile, a study of sea level response to the fluctuations in the local atmospheric factors has received less attention, and limited studies have highlighted this issue. Sharaf El Din (1990) studied the sea level variations on the western coast of the Arabian Gulf based on daily averages. He demonstrated that the sea level is generally low in winter and high in spring and summer. Sultan et al. (1995) studied sea level variations at the Saudi coast, west coast of the Arabian Gulf. They demonstrated that the range of monthly averages of sea level reaches 0.26 m. They also indicated that about 75% of this change was attributed to the fluctuation in the local AP, whereas the remaining signal could be due to density changes (steric effect). Hosseinibalam et al. (2007) addressed the interannual variability of sea level in the Iranian side, east coast of the Arabian Gulf. They showed that

the AP is responsible for 62–90.2% of seasonal variation in sea level; however, including the thermosteric sea level rise could improve the variance to 78.1–90.7%. Al-Subhi (2010) studied characteristics of the sea level at Juaymah on the west coast of the Arabian Gulf. He showed that the astronomical tide is responsible for about 90% of annual changes and the other 10% can be attributed to AP, water density, and wind stress. Afshar-Kaveh et al. (2020) examined the relationship between sea level fluctuation and meteorological elements along the east coast of the Arabian Gulf. They concluded that the low-frequency changes (the nontidal signal reaching 0.75 m) correlated with the corresponding fluctuation in air pressure and wind stress. Furthermore, they demonstrated that the impact of wind stress was higher than the effect of AP in their studied area. At this juncture, to the best of the author's knowledge, no studies highlighted the impact of changes of the atmospheric factors on the sea-surface fluctuations in the northwest tip of the Arabian Gulf. AlOsairi et al. (2018) conducted a harmonic analysis on water level records in Kuwait Bay. They demonstrated that astronomical tide is responsible for about 95% of sea level variations, whereas the changes in RWL are due to other factors. Lafta et al. (2019) studied the characteristics of the tidal wave in Khor Abdullah and Khor Al-Zubair, located in the northwest tip of the Arabian Gulf. They indicated that about 96% of annual variations in this region are due to the astronomical tide. However, they did not explain the reasons for the rest of the nontidal changes and the monthly weights of the tidal and nontidal signals. Hence, the present study aims to quantify the impacts of the atmospheric forces on the sea-surface fluctuations in the northwest tip of the Arabian Gulf. For fulfilling this objective, water levels and meteorological parameters (AP, AT, and wind speed and direction) records of the Iraq marine water were used.

Fig. 1 Location map of the study area showing the measurement station



Materials and methods

Study area

Iraq marine water is especially important as it represents the only way toward the sea for the country. The region appears as an estuarine environment located in the northwest tip of the Arabian Gulf (Al-Mahdi et al. 2009; Al-Taei et al. 2014).

The Arabian Gulf tidal regime is complex and varies spatially between diurnal, semidiurnal, and mixed tides. The tidal range is large and reaches 1 m in most locations of the gulf. This high tidal range is associated with strong tidal currents that exceed 0.5 m/s (Najafi 1997). The most important tidal constituents in Arabian Gulf are the semidiurnal M_2 and S_2 and diurnal K_1 and O_1 . Semidiurnal constituents have two amphidromic points, whereas the diurnal constituents have one amphidromic point (Reynolds 1993).

The climate of this region is characterized by an arid desert climate with two distinct seasons: a hot and long summer of about 230 days and cold and rainy winter (Zakaria et al. 2013). Rainfall occurs through the winter months, and its average is generally low with a negligible contribution to the water budget in Arabian Gulf (Reynolds 1993). High levels of AP characterize the Arabian Gulf during the winter. The highest values of AP occur in December and January. In contrast, the high air temperature (AT) through summer forms a low AP area covering the entire Arabian Gulf, with the lowest values during July (Sharaf El Din 1990). The prevailing wind regime in the northwest of the Arabian Gulf is the northwest wind, locally known as the Shamal wind. This wind blows on the area during most months of the year with notable seasonal variations. The second important wind regime in the region is the southeast wind (Kaus wind), and its period ranges from hours to several days, but its maximum speed is higher than the Shamal wind speed (Reynolds 1993).

Data sources

The study of long-term sea level variations in any region requires several years of recorded sea level data, whereas the study of seasonal changes can be conducted based on relatively short recorded data (Abdelrahman 1997). Generally, data for sea level measurements in Iraq marine water are scarce, especially after the Gulf War in the 1990s. In the past decade, Daewoo Engineering & Construction Co., Ltd., which constructed the western breakwater of Al-Faw port, installed a hydrographic station near the breakwater at $29^\circ 47.956'N$, $48^\circ 32.873'E$ (Fig. 1). It contained a tide gauge instrument and a weather station. An hourly record of the water level and meteorological parameters (AP, AT, and wind speed and direction) for the entire year of 2017 was accumulated from the Al-Faw station. The water level measurements were

rectified to the local vertical datum known as Faw 1979 (the mean sea level in this region).

The variations in AT can cause fluctuations in the sea-surface since they can influence several elements that participate in the sea level changes. Water expands when its temperature rises as a result of thermal expansion (IPCC 2013). Moreover, AT was chosen for quantifying the changes in sea level due to the lack of salinity and water temperature measurements.

Quantifying the influence of the atmospheric forces on the sea-surface fluctuations requires removing the tidal signal from the original water level data, commonly conducted by performing a harmonic analysis of the tide. The main important feature of the tidal harmonic analysis is distinguishing between the tidal and nontidal (RWL) signals. RWL is attributed to forces other than the tidal force (Al-Subhi 2010; Zubier 2010; Nhan 2016; Madah 2020). The Matlab World Tide, a package for analysis and prediction of the tide (Boon 2006), was used in the current study.

The wind vectors are divided into along-shore and cross-shore winds depending on the direction of the coast. However, the components of wind stress were calculated following the relation ($\tau_{u,v} = C_D \rho_a w_{10}^2$) given by Welander (1961), where $\tau_{u,v}$ are the components of wind stress, w_{10} is the wind speed measured at 10 m above the sea-surface, ρ_a is a density of air and equal to 1.3 kg/m^3 , and C_D is the wind drag coefficient with a value of 0.0026.

The daily averages of the RWL were obtained by averaging the resulting hourly RWL from the harmonic analysis, while those of meteorological elements were obtained by averaging their original, hourly recorded data. Furthermore, the monthly averages of these variables were obtained by simply averaging their daily averages.

Results

Water level measurements in the Iraq marine water displayed noticeable variations ranging from hourly to annual fluctuations due to several factors. The hourly sea level records showed a maximum range of about 4.33 m, oscillating from 1.64 to -2.69 m (Fig. 2). This range represents the largest range recorded in the entire Arabian Gulf water, as indicated by AlOsairi et al. (2018) and Lafta et al. (2020). In general, the hourly variations in the sea level can be related to the tidal effect. The harmonic analysis results of water level (Table 1) pointed out that the main astronomical tidal constituents (K_1 , O_1 , P_1 , M_2 , S_2 , N_2 , and K_2) explain about 90% of annual variances of water level fluctuations in the studied area. In contrast, the other 10% (RWL) can be attributed to other factors such as meteorological forces. A similar result was observed on the western coast of the Arabian Gulf (Al-Subhi 2010).

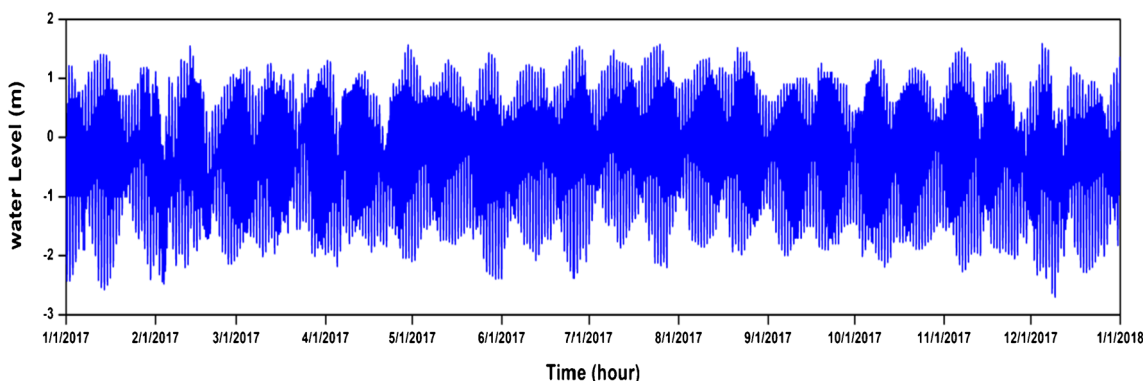


Fig. 2 Time series of hourly observed water level in the studied area during 2017

The monthly weights of the astronomical and meteorological tides were calculated based on their contribution to the original water level data as an average for each month according to the following relations (Tonbol and Shaltout 2013):

Tidal weights

$$= \frac{|monthly\ tidal\ average|}{|monthly\ tidal\ average| + |monthly\ nontidal\ average|} \times 100\%;$$

Meteorological tide weights

$$= \frac{|monthly\ nontidal\ average|}{|monthly\ tidal\ average| + |monthly\ nontidal\ average|} \times 100\%$$

Table 2 shows the results of these calculations. The tidal weight varies month by month. Moreover, tidal weight is the most major contributor to the sea level variations throughout the year, whereas the meteorological tide displayed a relatively considerable contribution during the winter and summer months. The highest contribution of the meteorological tide starts from late autumn to mid-winter and then drops to its lowest contribution level in late winter. Then, it has pronounced contribution in the summer, particularly during July when it reaches the maximum limit. This oscillation in the

meteorological tide could be mainly associated with variations in the local meteorological forces. Hence, further investigations are warranted to assess the influence of these forces on sea-surface fluctuations in this region.

Descriptive statics

Descriptive statistics were employed to recognize the annual and seasonal (91 days for each season) changes in the daily averages of RWL and the corresponding meteorological parameters.

Daily averages of RWL revealed pronounced annual, semi-annual, and seasonal fluctuations with the maximum and minimum heights during summer and winter, respectively. The maximum range reaches 1.08 m (Fig. 3A; Table 3); fluctuations of 0.75 m and 0.84 m were observed in the eastern and western sides of the Arabian Gulf, respectively (Afshar-Kaveh et al. 2020; Sultan et al. 2000). The seasonal variations in the RWL start to rise from late spring and then start declining in late autumn. Similar behavior of the seasonal sea level changes in the eastern and western coasts of the Arabian Gulf was

Table 1 Tidal constants for the main constituents from the harmonic analysis

Constituent	Period (h)	Amplitude (m)	Phase (degree)
O ₁	25.82	0.334	207.81
K ₁	23.93	0.515	296.21
P ₁	24.06	0.158	307.73
M ₂	12.42	0.936	271.72
S ₂	12	0.314	27.97
N ₂	12.69	0.195	158.26
K ₂	11.97	0.111	183.36

Table 2 The monthly weights of the astronomical tide and meteorological tide

Month	Astronomical tide (%)	Meteorological tide (%)
January	86.824	13.176
February	78.936	21.064
March	97.965	2.035
April	87.854	12.146
May	94.937	5.063
June	92.828	7.172
July	74.36	25.64
August	79.921	20.079
September	98.26	1.74
October	97.12	2.88
November	98.48	1.52
December	81.46	18.54

Table 3 Annual and seasonal statistical analyses (maximum, minimum, mean, and standard deviation) of RWL and atmospheric parameters

Parameters	Statics	Annual	Season			
			Winter	Spring	Summer	Autumn
Residual water level (m)	Max	0.426	0.380	0.269	0.426	0.206
	Min	-0.659	-0.659	-0.527	-0.119	-0.598
	Mean	-0.00015	-0.063	0.0031	0.112	-0.054
	Stdv	0.169	0.18	0.150	0.124	0.161
Atmospheric pressure (hPa)	Max	1027.68	1027.68	1017.67	1009.94	1025.69
	Min	993.06	1007.66	995.25	993.06	1008.54
	Mean	1009.84	1017.14	1006.1	1000.04	1016.2
	Stdv	8.4	4.95	4.21	4.15	4.35
Air temperature (°C)	Max	40.24	22.72	37.55	40.24	34.09
	Min	8.25	8.25	22.31	27.75	14.64
	Mean	26.13	15.4	30.67	34.77	23.51
	Stdv	8.48	3.93	4.34	2.53	5.54
Along-shore wind stress (N/m²)	Max	-0.2308	-0.185	-0.2308	-0.143	-0.116
	Min	-54×10^{-7}	-54×10^{-7}	15×10^{-5}	1×10^{-6}	7×10^{-6}
	Mean	-0.0094	-0.0079	-0.027	0.0021	-0.0047
	Stdv	0.047	0.047	0.059	0.034	0.04
Cross-shore wind stress (N/m²)	Max	0.309	0.185	0.309	0.200	0.206
	Min	1×10^{-6}	-1×10^{-5}	69×10^{-5}	1×10^{-6}	-68×10^{-6}
	Mean	0.023	0.014	0.042	0.012	0.023
	Stdv	0.059	0.055	0.075	0.038	0.057

observed, with a different range of oscillation (Sultan et al., 1995; Afshar-Kaveh et al. 2020). Furthermore, depending on the standard deviation values, the time series of RWL daily averages indicated a noticeable increase in oscillation amplitude in winter and autumn and a small oscillation in summer and spring. Such behavior was observed in the central part of the Red Sea (Sultan and Elghribi 2003). Correspondingly, the atmospheric parameters exhibited noticeable variations both seasonally and annually (Fig. 3B–E). AP reached its maximum and minimum limits during winter and summer, respectively. The highest amplitude of oscillation in AP occurred in winter and autumn, while the minimum occurred in summer and spring (Fig. 3B).

Meanwhile, the maximum and minimum limits of AT occurred in summer and winter, respectively. The highest oscillation range of AT was in autumn and spring and the lowest in summer and winter, as indicated by standard deviation values (Table 3). Correspondingly, the maximum and minimum values of ASWS occurred during spring and winter, respectively. The highest oscillation range in ASWS was in spring and winter and the lowest in summer and autumn, as indicated by the standard deviation values (Table 3). Moreover, CSWS reached the maximum limit in spring and the minimum in summer (Table 3). According to standard deviation values, the highest oscillation range in CSWS occurs in spring and autumn and the lowest in summer and winter. It is worth

mentioning that the positive and negative values of ASWS refer to the northwards and southwards directions, respectively, while the positive and negative values of CSWS refer to the eastwards and westwards directions, respectively.

Spectral analysis

Spectral analysis based on the fast Fourier transform (FFT) of the daily averages for RWL and meteorological parameters (AP, AT, and wind stress components) was conducted. Figure 4 displays the energy spectrum distribution between the different frequencies for RWL and the meteorological parameters. The time series of these variables were divided into 182 frequencies based on the original data sets. The lower frequency of these ranges was at 3.17×10^{-8} Hz (or 0.00274 CpD) and the upper frequency at 5.78×10^{-6} Hz (or 0.5 CpD), with an interval of 3.17×10^{-8} Hz. These frequencies are equivalent to about 2–365 days. However, for every specific frequency, the amplitude and phase were quantified.

Spectral analysis results for RWL indicated that the significant energy peak corresponds to its annual frequency, which is equivalent to a period of 365 days, followed by the semi-annual frequency at 6.34×10^{-8} Hz and several peaks correspond to other low frequencies until 2.89×10^{-6} Hz. The energy spectrum decreases toward the higher frequencies (Fig. 4A). Meanwhile, the energy spectra for both AP and AT

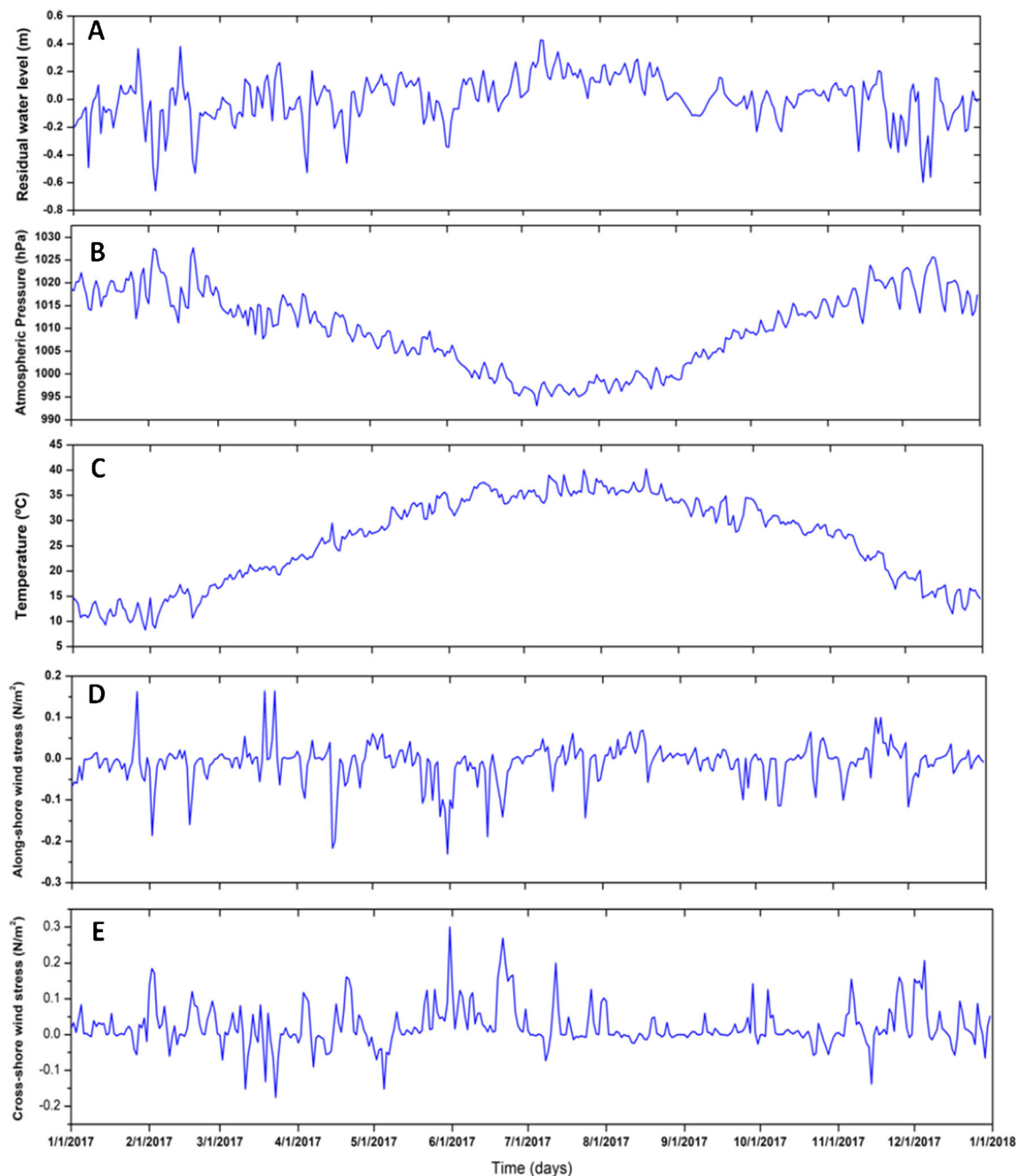


Fig. 3 The daily averages for RWL (A) and the corresponding atmospheric parameters (B–E)

exhibited sharp peaks at their annual frequency and small ones at the semiannual frequency (Fig. 4B,C).

Conversely, the energy spectrum of ASWS revealed that the significant peak does not concentrate at its annual frequency; rather, it corresponds to the frequency of 9.51×10^{-8} Hz or 121.25 days. Then, several peaks correspond to frequencies ranging from 1.26×10^{-7} to 5.78×10^{-6} Hz, with the most significant peaks being equivalent to 60.82 days, 52.13 days, 33.17 days, 20.2 days, 14.6 days, 5.2 days, and 5.06 days (Fig. 4D). Correspondingly, the CSWS spectrum demonstrated two sharp peaks concentrated at both the semiannual frequency as

well as at 5.708×10^{-7} Hz, which is equivalent to 20.2 days (Fig. 4E). Furthermore, several peaks appeared in the energy spectrum of CSWS, but the most significant were concentrated at frequencies equivalent to 60.82 days, 33.17 days, 28 days, 19.2 days, 15.2 days, 10.7 days, and 5 days.

Regression analysis

Regression analysis was carried out to investigate further the response of RWL to atmospheric forces based on the monthly and seasonal averages (91-day period for every season).

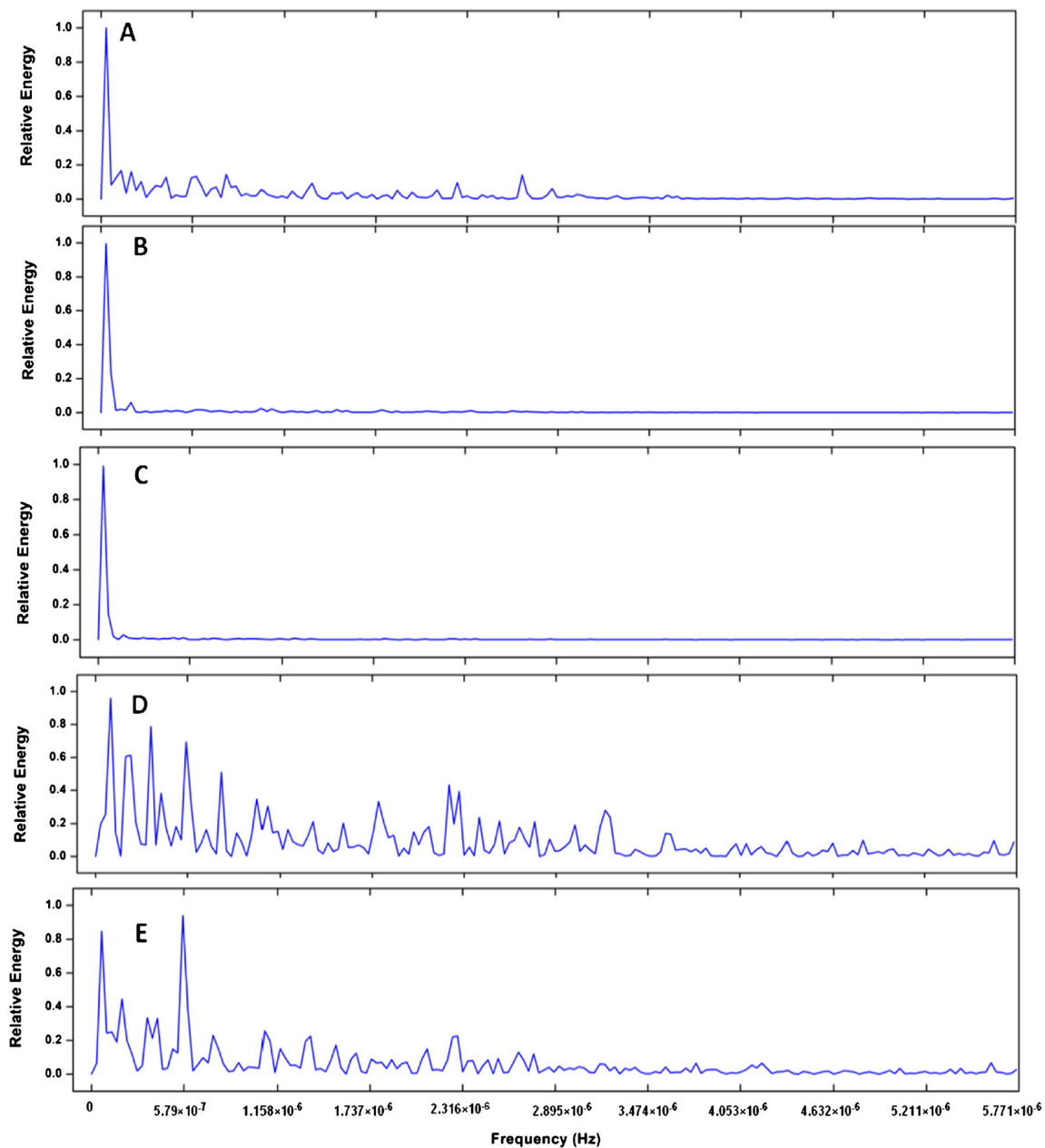


Fig. 4 Distribution of energy spectrum between various frequencies for residual water level (**A**), atmospheric pressure (**B**), air temperature (**C**), along-shore wind stress (**D**), and cross-shore wind stress (**E**)

Figure 5 displays the monthly averages for RWL, AP, AT, ASWS, and CSWS. The calculation of the regression parameters was conducted with a 95% confidence interval. However, the changes in monthly averages of RWL gave an annual range of about 0.36 m for the sea level in the northwest tip of the Arabian Gulf. The maximum and minimum heights of RWL appear during summer (July) and winter (February), respectively (Fig. 5A).

Correspondingly, the monthly averages of AP displayed a pronounced annual cycle with the highest values during winter, i.e., December with 1019.842 hPa, and the lowest values during summer, i.e., July with 996.59 hPa (Fig. 5B). In contrast, the

monthly averages of AT fluctuated between the highest values during summer and reached about 36.5°C and then dropped to the lowest values in winter at 14.5°C (Fig. 5C). Meanwhile, the analysis of recorded wind speed implied that it reached maximum speed during late spring and early summer (Fig. 5D). The dominant direction of the monthly averages of the ASWS is southwards (negative values) during most months except in winter (January and March) and summer (positive values). On the other hand, the CSWS is directed eastwards (positive values) throughout the year except in January and March, and when the southeast wind dominates in the region, it is directed westwards (negative values) (Fig. 5E).

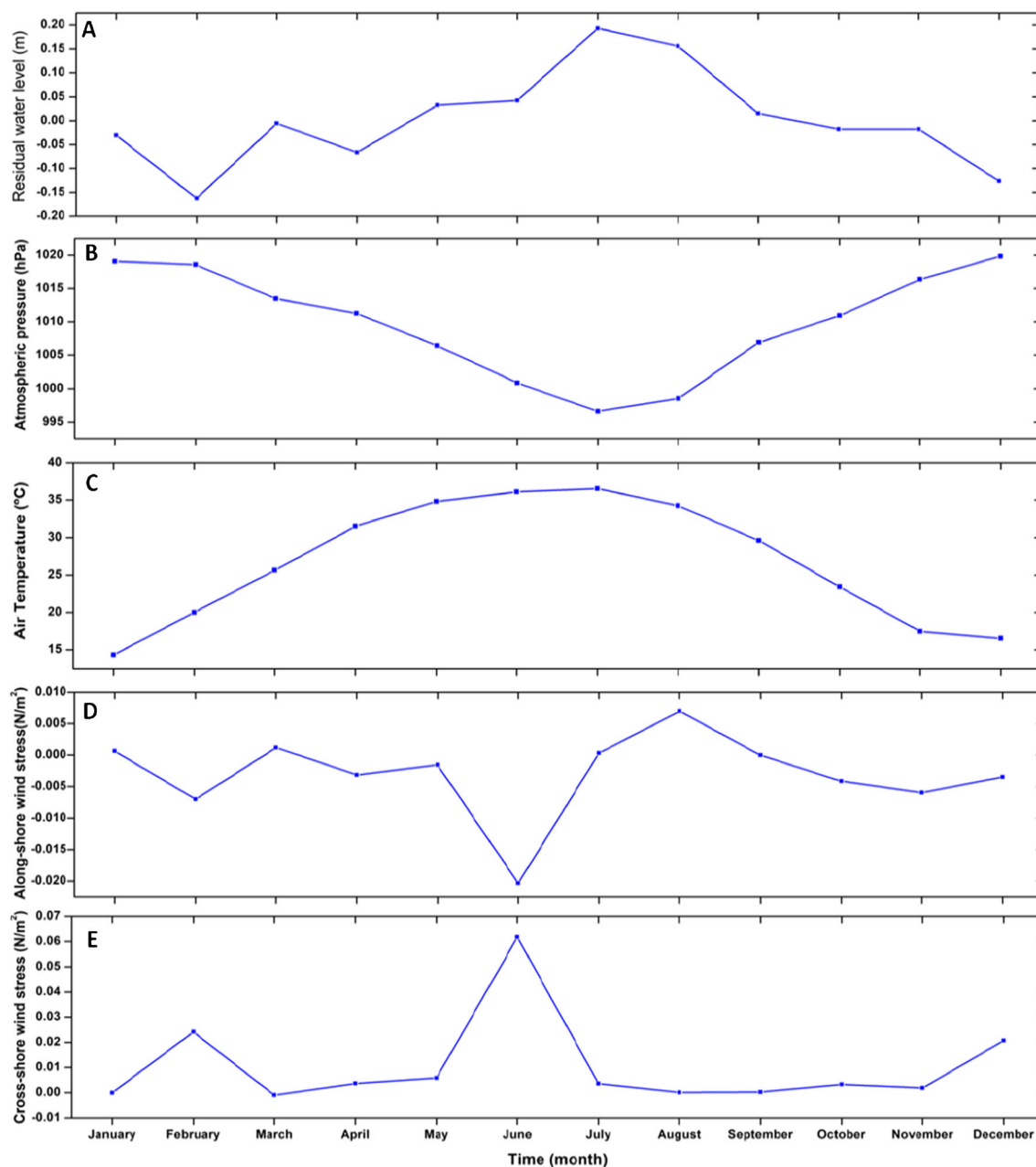


Fig. 5 Monthly averages for RWL (A) and the corresponding atmospheric parameters (B–E)

Discussion

The statistical analysis results revealed that RWL and all the corresponding atmospheric parameters displayed various changes throughout the year; that is, they exhibited several patterns of variations ranging from seasonal changes to relatively short-term changes within each season (Fig. 3). The maximum/minimum increase/decrease in the RWL seasonal averages above the annual average was in the summer and winter seasons, respectively. The difference in the seasonal means of RWL between summer and winter was about 0.18 m (Table 3). The increase of the oscillation amplitudes of

RWL during the winter and autumn seasons was mainly correlated with the apparent rise in the AP oscillation range during this time, particularly in winter. In contrast, the increase in the AT oscillation range in autumn seemed to enhance the fluctuation pattern of the RWL behavior.

Spectral analysis results (amplitudes and phases in addition to the percent of variance) for the most significant frequencies that correspond to the periods of 365 days, 182.25 days, 121.65 days, 91.24 days, 60.82 days, 52.13 days, 45.62 days, 36.49 days, and 33.17 days are shown in Table 4. The amplitudes of RWL for both annual and semiannual cycles obtained by the spectral analysis are comparable to those observed on

the western side of the Arabian Gulf (Sultan et al. 1995; Sultan et al. 2000).

However, the frequencies group ranged from 3.8×10^{-7} to 5.78×10^{-6} Hz, equivalent to 30 to 2 days; hereafter, we call it high-band frequencies (HBFs). These frequencies appear to have a significant contribution in both RWL and meteorological parameters spectra. Table 5 shows the percent of variance for the high-band residual water level (HB RWL) and the meteorological parameters. From Tables 4 and 5, only about 21% of the RWL variation is due to the annual cycle, whereas more than 60% of RWL variations have coincided with HB RWL. Furthermore, the rest frequencies, equivalent to the period between 182.5 and 33.17 days, participated with about 18.2% of the total variance in the RWL spectrum. Hence, the time scale of RWL variations is ranging from about 2 days to 1 year.

The HB RWL was obtained by applying a high-pass filter for the RWL daily averages with a cutoff frequency at 3.85×10^{-7} Hz. Similarly, the HBFs for the meteorological parameters were obtained by applying the same filter for their daily averages. The HB RWL changes seasonally; it is higher in the winter than in the summer (Fig. 6A). However, HB RWL seems to precisely behave oppositely to the original RWL, increasing in the summer and decreasing in the winter. Such behavior pattern of HB RWL could be attributed to the impact of wind activity in this range of time, which masked the effects of other forces. The HBFs for both components of wind stress seem to be similar to their original daily averages (Fig. 6D,E). Hence, the annual changes in the wind stress components could be neglected compared to the greater changes that coincided with their HBFs.

The comparison of HBFs for both AP and AT with their original daily averages confirmed that their highest variations were basically due to the annual cycles (Fig. 6B,C). Moreover, the comparison of the original daily averages of AP with HB AP indicated that this parameter had the lowest oscillation range during spring and summer and highest during winter and autumn (Fig. 6B), confirming the aforementioned results found by the standard deviation values for AP (Table 3). Correspondingly, the AT annual variance had the greatest contribution in its spectrum and reached about 94% of the total variance, while other cycles seemed to have an insignificant effect.

The comparison between RWL and AP in terms of phases (Table 4) indicated that these two variables are clearly inversely correlated at the annual cycle. Such a cycle accounts for more than 87% of the total variance in AP. Hence, the AP participated significantly in the annual variation of RWL. Meanwhile, the HBFs AP accounted for only about 7.5% of the atmospheric pressure variations. Comparing RWL and AT in terms of phase revealed that they almost coincided at an annual frequency, whereas no direct relation existed with other cycles. Consequently, the increase in the contribution percentage of the meteorological tide in the observed water level during summer and winter (Table 2) could be mainly attributed to the annual variations in both AP and AT.

Furthermore, more than 76% of the variance for both components of the wind stress was associated with the HBFs cycle (Table 5). For the ASWS, the annual cycle seemed not to have any contribution to the total variance. On the other hand, the frequencies equivalent to 121.65 days and 33.17 days exhibited a minor contribution of 5.5% and 4.5%, respectively.

Table 4 Amplitude, phase, and percentage of variance for significant frequencies for RWL and atmospheric parameters

Variables	Parameters	Frequency (Hz)									
		3.17×10^{-8}	6.34×10^{-8}	9.51×10^{-8}	1.26×10^{-7}	1.90×10^{-7}	2.21×10^{-7}	2.53×10^{-7}	3.17×10^{-7}	3.48×10^{-7}	
Residual water level	Amp (m)	0.1105	0.031	0.038	0.045	0.044	0.024	0.035	0.024	0.031	
	Phs (degree)	163.87	305.62	133	262.26	311.39	203.94	64.21	222.32	62.42	
	Var (%)	21.23	1.75	2.63	3.53	3.39	1.04	2.17	1.03	1.68	
Atmospheric pressure	Amp(hPa)	11.08	2.19	0.52	0.63	1.12	0.26	0.2	0.1	0.33	
	Phs (degree)	-111.77	120.47	259.37	179.19	163.26	40.28	-49.03	-158.52	-236.25	
	Var (%)	87.2	3.42	0.19	0.28	0.89	0.04	0.03	0.07	0.07	
Temperature	Amp (°C)	11.59	1.752	0.62	0.15	0.46	0.38	0.33	0.31	0.39	
	Phs (degree)	158.31	130.18	148.83	174.64	46.18	13.96	47.39	114.44	-10.42	
	Var (%)	93.63	2.13	0.270	0.01	0.14	0.1	0.1	0.07	0.07	
Along-shore wind stress	Amp (N/m ²)	0.007	0.008	0.015	0.006	0.012	0.012	0.007	0.004	0.014	
	Phs (degree)	60.56	-117.23	-273.03	-148.8	-41.78	-161.62	-291.02	-85.73	-269.18	
	Var (%)	1.12	1.47	5.51	0.84	3.47	3.51	1.2	0.404	4.53	
Cross-shore wind stress	Amp(N/m ²)	0.006	0.022	0.012	0.012	0.016	0.01	0.008	0.005	0.014	
	Phs (degree)	-161	-330.71	-127.07	-254.42	-209.57	-28.53	-98.08	-323.15	-70.35	
	Var (%)	0.55	7.28	2.1	2.14	3.82	1.71	0.99	0.41	2.87	

Table 5 Percent of variance explained by high-band frequencies (3.8×10^{-7} to 5.78×10^{-6} Hz) for RWL and atmospheric parameters

Variable	Residual water level	Atmospheric pressure	Air temperature	Alongshore wind stress	Cross-shore wind stress
Variance (%)	60.4	7.5	2.8	76.94	76.07

Conversely, the semiannual cycle for the CSWS seemed to have a little contribution to the total variance, with a percentage exceeding 7%. Corresponding to the annual cycle, comparing RWL and ASWS in terms of phases (Table 4)

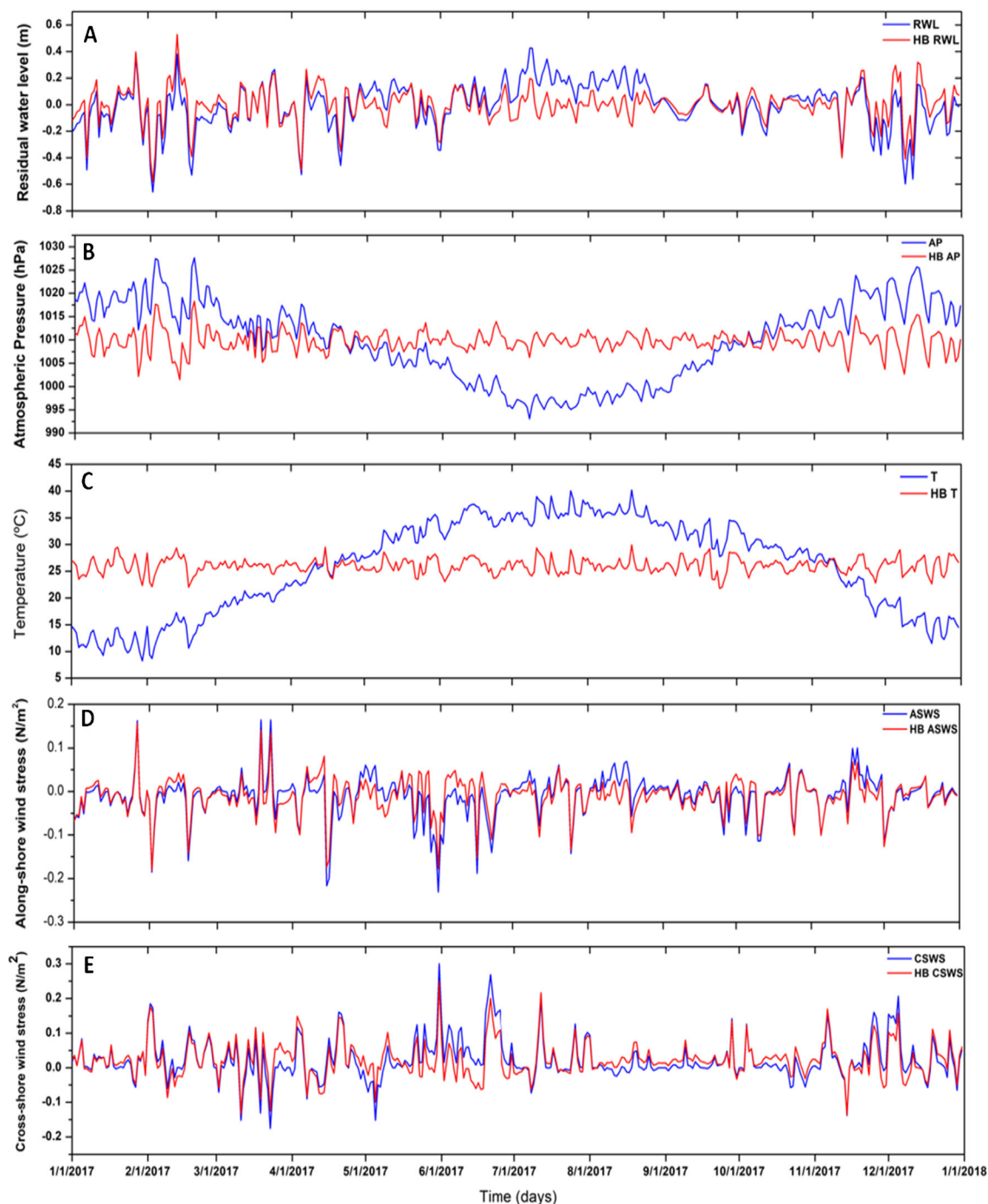


Fig. 6 Comparison of the original daily averages (blue) with high-band frequencies group (red) for RWL (A) and the corresponding atmospheric parameters (B–E)

revealed the presence of the phase lag between these two variables; however, the relationship between them is more positive. Regarding the CSWS, the two variables appear to be inversely correlated (180 out of phase). However, based on the higher variance percentage associated with the HBFs for RWL and both components of wind stress, it is evident that the fluctuations in RWL in this range of time basically coincided with the wind regime in the area.

Moreover, based on the regression analysis results, the comparison of monthly averages for RWL and AP indicated that the two variables are inversely related (Table 6). The theoretical hypothesis about the sea-surface and AP assumes that with every 1 hPa increase in air pressure, the sea-surface is lowered by 0.01 m and vice versa (Roden and Rossby 1999). The calculations indicated a high correlation between the monthly averages for RWL and AP with a correlation coefficient of -0.89 . The regression coefficient of 0.011 m/hPa is approximately equal to the value supposed by the theoretical hypothesis. Unlike the response of the sea level in the Red Sea to AP, the sea-surface in the northwest tip of the Arabian Gulf, on a monthly basis, responds to AP approximately as an inverse barometer. A similar result was observed in the western coast of the Arabian Gulf (Sultan et al. 1995; Sultan et al. 2000). The comparison of the monthly averages for RWL and AT indicated a positive correlation between them (Table 6). The regression analysis between these two elements resulted in a correlation coefficient of 0.7 . The comparison of monthly averages of RWL and ASWS implied a positive correlation (Table 6), meaning the southward wind lowers the

sea-surface, whereas the northward wind raises it. Obviously, the southward components of the wind stress appear to depress the sea-surface of the Arabian Gulf by dragging the water masses toward the Gulf of Oman. In contrast, the northward component has an opposite action and acts to raise the sea-surface in the Arabian Gulf. As for the CSWS, a negative correlation coefficient with RWL was observed (Table 6). Eastward wind lowers thesea-surface, whereas the westwards wind raises it.

However, the regression analysis based on the seasonal variations (short-term changes) exhibited a significant difference in the response of RWL to variations in atmospheric parameters between seasons. In winter, a relatively high correlation existed between RWL and AP, CSWS, and ASWS, respectively (Table 6). The regression coefficient between AP and RWL of 0.028 m/hPa showed that there was a high response of RWL to this variable and that the RWL changes are about three times those predicted by the theoretical hypothesis. In winter, the high air pressure area covers the entire Arabian Gulf, coinciding with the decrease in AT, leading to a significant depression in the sea-surface in the Arabian Gulf. Furthermore, both ASWS and CSWS seem to have a relatively significant effect on RWL during this season, particularly in February, when RWL is clearly lowered (see Fig. 5A). This corresponds to a relatively high southward ASWS and eastward CSWS, so the decrease in RWL could be attributed to the effect of AP and the wind pattern in this period.

Furthermore, during spring, minor effects of both AP and AT on RWL were observed, confirmed by a relatively low

Table 6 Regression analysis for RWL and the corresponding atmospheric parameters based on the seasonal and monthly averages

Parameter	Statics	Analysis basis				
		Monthly means	Season			
			Winter	Spring	Summer	Autumn
Atmospheric pressure	Regression equation	11.253–0.011 AP	28.461–0.028 AP	14.158–0.014 AP	19.235–0.019 AP	7.678–0.0076 AP
	Correlation	-0.89	-0.65	-0.46	-0.64	-0.52
	Standard error	0.048	0.136	0.134	0.095	0.158
Air temperature	Regression equation	$-0.23+0.0086$ AT	$-0.322+0.016$ AT	$-0.299+0.0098$ AT	$-0.755+0.024$ AT	$-0.334+0.011$ AT
	Correlation	0.7	0.36	0.28	0.5	0.4
	Standard error	0.075	0.168	0.1455	0.107	0.147
Along-shore wind stress	Regression equation	0.01+4.63 ASWS	$-0.048+1.79$ CSWS	0.038+1.3 CSWS	0.109+1.32 CSWS	$-0.051+0.603$ CSWS
	Correlation	0.3	0.47	0.51	0.36	0.48
	Standard error	0.10	0.15	0.13	0.11	0.16
Cross-shore wind stress	Regression equation	0.01–0.95 CSWS	$-0.035–1.91$ CSWS	0.048–1.07 CSWS	0.119–0.58 CSWS	$-0.046–0.35$ CSWS
	Correlation	-0.17	-0.59	-0.53	-0.18	-0.44
	Standard error	0.10	0.14	0.12	0.12	0.16

correlation coefficient (Table 6). In early spring, the RWL appears to be low (Fig. 5A), although it starts to increase in late winter. The lowering of RWL could be particularly associated with the intensification of the southward ASWS and eastward CSWS at this time, confirmed by the increased correlation coefficients between RWL and wind components in this period (Table 6). In late spring, minor effects of the wind stress components on RWL were observed. The southward ASWS and eastward CSWS reached their maximum limits during June, whereas RWL was not affected by the increase in the wind components, which was expected to lower RWL, due to the increased influence of both AP and AT in late spring. Hence, the effect of the wind pattern could be masked by the increasing effect of both AP and AT during this time.

Moreover, during summer, a relatively high correlation was observed between RWL and both AP and AT (Table 6). A combined effect of AP and AT, which reached their minimum and maximum limits, respectively, during July, in addition to the ASWS directed northwards, enhanced RWL for a rising to its highest limit at this period. In late summer, AP began to rise again, while AT seemed to decrease and ASWS direction returned southwards. The changes in these influencing parameters led to the rapid decrease in RWL from mid to late summer. Furthermore, the RWL seemed to be steady during early autumn, and then, starting from the mid-season, it dropped rapidly. However, during mid-to-late autumn, a rapid increase in AP and a rapid decrease in AT were observed (see Fig. 5). Correspondingly, the southwards ASWS started to weaken, whereas the eastwards CSWS seemed to strengthen during the second half of the season. This pattern of variations in these influencing factors led to a considerable drop in the RWL during late autumn.

Conclusions

Harmonic analysis results of water-level records in the Iraq marine water revealed that the tidal phenomena were responsible for about 90% of the annual variation of the sea-surface, whereas the rest of the changes are mainly related to the impact of atmospheric forces on the region. The relative contribution of the astronomical and meteorological tides in the observed water level varies monthly and seasonally.

Statistical and spectral analyses for the daily and monthly averages of RWL and atmospheric parameters showed the presence of annual and relatively short-term variations. The maximum ranges for daily and monthly averages RWL were 1.08 m and 0.36 m, respectively. The highest and lowest limits of RWL were in summer and winter, respectively.

Short-term variations of RWL have basically coincided with the HBFs for ASWS and CSWS. Therefore, the effect of the wind regime in the region could be responsible for the short-term variations in RWL. At the same time, the annual

variation in RWL has mainly coincided with the changes in the AP and AT.

Furthermore, the regression results indicated that the influence of the individual atmospheric parameters on RWL varies seasonally. The maximum and minimum effects of AP on RWL were during winter and spring, respectively. Correspondingly, the maximum and minimum effects of AT on the RWL were during summer and spring, respectively. Meanwhile, the maximum and minimum effects of ASWS were during spring and summer, respectively, whereas those of CSWS were during winter and summer, respectively. It is worth noting that the results obtained in this study were based on relatively short data records. Hence, the availability of long data records in the future could give a more accurate description of the behavior of the sea-surface fluctuations in this region.

Acknowledgements The author is grateful to Daewoo Engineering & Construction Company for technical support and for providing valuable data sets in this region.

Availability of data and material Not applicable

Code availability <http://www.mathworks.com/matlabcentral/fileexchange/24217-world-tides>

Declarations

Conflict of interest The author declares no competing interest.

References

- Abdelrahman SM (1997) Seasonal fluctuations of mean sea level at Gizan, Red Sea. *J Coast Res* 13:1166–1172 <https://www.jstor.org/stable/4298725>
- Afshar-Kaveh N, Nazarali M, Pattiaratchi C (2020) Relationship between the Persian Gulf sea-level fluctuations and meteorological forcing. *J Mar Sci Eng* 8:285. <https://doi.org/10.3390/jmse8040285>
- Al-Mahdi AA, Abdullah SS, Husain NA (2009) Some features of the physical oceanography in Iraqi marine water. *Mesopotamian J Mar Sci* 24:13–24
- AlOsairi Y, Imberger J, Falconer RA (2011) Mixing and flushing in the Persian Gulf (Arabian Gulf). *J Geophys Res* 116:C03029. <https://doi.org/10.1029/2010JC006769>
- AlOsairi Y, Pokavanich T, Alsulaiman N (2018) Three-dimensional hydrodynamic modeling study of reverse estuarine circulation: Kuwait Bay. *Mar Pollut Bull* 127:82–96. <https://doi.org/10.1016/j.marpolbul.2017.11.049>
- Alothman A, Ayhan M (2010) Detection of sea level rise within the Arabian Gulf using space based GNSS measurements and in situ tide gauge data. *38th COSPAR Scientific Assembly* 38:3–7
- Al-Subhi AM (2010) Tide and sea level characteristics at Juaymah, west coast of the Arabian Gulf. *J King Abdul-Aziz Univ-Mar Sci* 21: 133–149. <https://doi.org/10.4197/Mar.21-1.8>
- Al-Taei SA, Abdulla SS, Lafta AA (2014) Longitudinal intrusion pattern of salinity in Shatt Al Arab estuary and reasons. *J King Abdul-Aziz Univ-Mar Sci* 25:205–221. <https://doi.org/10.4197/Mar.25-2.10>

- Boon JD (2006) World tides user manual v1. 01, USA, 24p
- Boon JD (2013) Secrets of the tide: tide and tidal current analysis and predictions, storm surges and sea level trends. Elsevier. (224 pp)
- Hosseiniabalam F, Hassanzadeh S, Kiasatpour A (2007) Interannual variability and seasonal contribution of thermal expansion to sea level in the Persian Gulf. *Deep-Sea Res I Oceanogr Res Pap* 54:1474–1485. <https://doi.org/10.1016/j.dsr.2007.05.005>
- IPCC (2013) Climate change: the physical science basis: Working Group I contribution to the fifth assessment report of the Intergovernmental Panel on Climate Change. Cambridge University Press
- Kämpf J, Sadrinab M (2006) The circulation of the Persian Gulf: a numerical study. *Ocean Sci* 2:27–41. <https://doi.org/10.5194/os-2-27-2006>
- Lafta AA, Altaei SA, Al-Hashimi NH (2019) Characteristics of the tidal wave in Khor Abdullah and Khor Al-Zubair channels, northwest of the Arabian Gulf. *Mesopot J Mar Sci* 34:12–125
- Lafta AA, Altaei SA, Al-Hashimi NH (2020) Impacts of potential sea-level rise on tidal dynamics in Khor Abdullah and Khor Al-Zubair, northwest of Arabian Gulf. *Earth Syst Environ* 4:93–105. <https://doi.org/10.1007/s41748-020-00147-9>
- Li Y, Han W (2015) Decadal sea level variations in the Indian Ocean investigated with HYCOM: roles of climate modes, ocean internal variability, and stochastic wind forcing. *J Clim* 28:9143–9165. <https://doi.org/10.1175/JCLI-D-15-0252.1>
- Madah FA (2020) The amplitudes and phases of tidal constituents from harmonic analysis at two stations in the Gulf of Aden. *Earth Syst Environ* 4:321–328. <https://doi.org/10.1007/s41748-020-00152-y>
- Najafi H S (1997) Modeling tides in the Persian Gulf using dynamic nesting. Ph.D. thesis, University of Adelaide, Adelaide, South Australia. <http://hdl.handle.net/2440/19562>
- Nhan NH (2016) Tidal regime deformation by sea level rise along the coast of the Mekong Delta. *Estuar Coast Shelf Sci* 183:382–391. <https://doi.org/10.1016/j.ecss.2016.07.004>
- Pugh DT, Woodworth PL (2014) Sea-level science: understanding tides, surges, tsunamis and mean sea level changes. Cambridge University Press, Cambridge
- Ranjbar MH, Etemad-Shahidi A, Kamranzad B (2020) Modeling the combined impact of climate change and sea-level rise on general circulation and residence time in a semi-enclosed sea. *Sci Total Environ* 740:140073. <https://doi.org/10.1016/j.scitotenv.2020.140073>
- Reynolds RM (1993) Physical oceanography of the Gulf, Strait of Hormuz, and the Gulf of Oman: results from the Mt Mitchell expedition. *Mar Pollut Bull* 27:35–59. [https://doi.org/10.1016/0025-326X\(93\)90007-7](https://doi.org/10.1016/0025-326X(93)90007-7)
- Roden GI, Rossby HT (1999) Early Swedish contribution to oceanography: Nils Gissler (1715–71) and the inverted barometer effect. *Bull Am Meteorol Soc* 80:675–682 <https://www.jstor.org/stable/26214922>
- Saad NN, Moursy ZA, Sharaf El Din SH (2011) Water heights and weather regimes at Alexandria Harbor. *Int J Phys Sci* 6:7035–7043. <https://doi.org/10.5897/IJPS11.018>
- Sadrinasab M, Kämpf J (2004) Three-dimensional flushing times of the Persian Gulf. *Geophys Res Lett* 31:1–4. <https://doi.org/10.1029/2004GL020425>
- Sharaf El Din SH (1990) Sea level variation along the western coast of the Arabian Gulf. *Int Hydrogr Rev* 67:103–109
- Siddig NA, Al-Subhi AM, Alsaafani MA (2019) Tide and mean sea level trend in the west coast of the Arabian Gulf from tide gauges and multi-missions satellite altimeter. *Oceanologia* 61:401–411. <https://doi.org/10.1016/j.oceano.2019.05.003>
- Stewart RH (2009) Introduction to physical oceanography. University Press of Florida, 353 p
- Sultan SA, Elghribi NM (2003) Sea level changes in the central part of the Red Sea. *Indian J Geo-Mar Sci* 32:114–122 <http://nopr.niscair.res.in/handle/123456789/4254>
- Sultan SA, Ahmed F, Elghribi NM, Al-Subhi AM (1995) An analysis of Arabian Gulf monthly mean sea level. *Cont Shelf Res* 15:1471–1482. [https://doi.org/10.1016/0278-4343\(94\)00081-W](https://doi.org/10.1016/0278-4343(94)00081-W)
- Sultan SA, Moamar MO, Elghribi NM, Williams R (2000) Sea level changes along the Saudi coast of the Arabian Gulf. *Indian J Geo-Mar Sci* 29:191–200 <http://nopr.niscair.res.in/handle/123456789/25532>
- Tonbol K, Shaltout M (2013) Tidal and non-tidal sea level off Port Said, Nile Delta. *Egypt J King Abdul-Aziz Univ-Mar Sci* 24:69–83. <https://doi.org/10.4197/Mar.24-2.5>
- Welander P (1961) Numerical prediction of storm surge. *Adv Geophys* 8: 315–379. [https://doi.org/10.1016/S0065-2687\(08\)60343-X](https://doi.org/10.1016/S0065-2687(08)60343-X)
- Willis JK, Chambers DP, Nerem RS (2008) Assessing the globally averaged sea level budget on seasonal to interannual timescales. *J Geophys Res-Oceans* 113:9. <https://doi.org/10.1029/2007JC004517>
- Zakaria S, Al-Ansari N, Knutsson S (2013) Historical and future climatic change scenarios for temperature and rainfall for Iraq. *J Civ Eng Archit* 7:1574–1594. <https://doi.org/10.17265/1934-7359/2013.12.012>
- Zubier KM (2010) Seal level variations at Jeddah, eastern coast of the Red Sea. *J King Abdul-Aziz Univ-Mar Sci* 21: 73-86. DOI : 10.4197/Mar. 21–2.6
- Zubier KM, Eyouni LS (2020) Investigating the role of atmospheric variables on sea level variations in the Eastern Central Red Sea using an artificial neural network approach. *Oceanologia* 62:267–290. <https://doi.org/10.1016/j.oceano.2020.02.002>